RICE UNIVERSITY

Black oil simulation utilizing a central finite volume scheme

by

Rujeko Chinomona

A Thesis Submitted
in Partial Fulfillment of the
Requirements for the Degree

Master of Arts

Approved, Thesis Committee:

Beatrice M. Riviere
Noah G. Harding Chair
Professor of Computational and Applied Mathematics

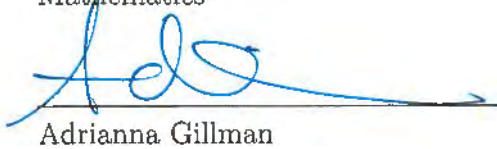

Adrianna Gillman
Assistant Professor of Computational and Applied Mathematics

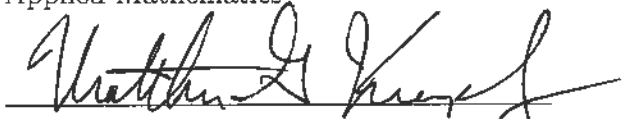

Matthew G. Knepley
Assistant Professor of Computational and Applied Mathematics

Houston, Texas

April, 2016

ABSTRACT

Black oil simulation utilizing a central finite volume scheme

by

Rujeko Chinomona

Black-oil simulation is a valuable tool in predicting the multi-phase multi-component flow of fluids in reservoirs. This research validates the use of a central high resolution finite volume scheme developed by Kurganov and Tadmor (KT) to the black-oil model problem. The KT scheme is desirable because of its relative ease of implementation and its ability to generate high resolution solutions at low computational costs. In addition, convergence rates on simple hyperbolic conservation law problems provided in this thesis indicate that the KT scheme is second order. Results obtained from simulations are in alignment with published literature and simulations also accommodate changing variables with predictable outcomes. The KT scheme can be applied to the black-oil model problem with increased confidence.

Acknowledgments

I am extremely grateful for Dr. Beatrice Riviere's excellent instruction, patience, and encouragement in making this thesis possible. I also extend my gratitude to Dr. Adrianna Gillman and Dr. Matt Knepley for mentoring me and reviewing this work. I am forever indebted to Dr. Jan Hewitt and Dr. Paul Hand for providing invaluable lessons in thesis writing and communicating my ideas effectively.

I am thankful for my amazing friends (those at Rice and those spread across the globe), they listened and remained supportive. I am grateful for Hannah Golub and the time she took to help me navigate life at Rice and beyond. Thanks to the CAAM faculty, staff, and my CAAM peers; especially Emily Hendryx whose mentorship I could not have done without. Special thanks to Bradley Johnson for being a wonderful friend, study buddy, and offering a different perspective on most matters.

My family has been the greatest support system through it all. This work would not have been possible without their inspiration, support, and belief in my potential.

Contents

Illustrations

Tables

Chapter 1

Introduction

1.1 Motivation

Oil and gas companies are interested in predicting pressure and compositional changes that occur in a reservoir. Predictions aid in the development of efficient drilling strategies for maximizing output and profits. Reservoir simulations are cost effective ways for oil and gas companies to determine the nature of the reservoir. A reservoir is a porous medium made up of solid material and void or gaps between the solid material. Components such as oil, gas, and water tend to accumulate in these gaps and they interact in different phases. Oil is usually in the liquid phase, gas is in the vapor phase and water is in the aqua phase since oil and gas do not mix. The multi-phase, multi-component flow of fluids in porous media can be modeled by systems of partial differential equations, for example the black-oil model ([4],[1],[5]).

The black-oil system of equations has been around for a number of decades and it is an important model to validate for researchers interested in developing new methods for multi-phase flow in porous media. In this thesis, a scheme originally presented by Kurganov and Tadmor [11] (KT scheme) is applied to the one dimensional black-oil model. This application of the KT scheme provides a validation for the results

according to Karimi et al.[8]. The second order accuracy of the KT scheme is verified by applying the scheme to simple hyperbolic conservation laws. Results show that the simulations of the black-oil model are adaptable to changing variables with predictable outcomes. The motivation in carrying out this work is to provide technical details of the implementation of the KT scheme that might have been otherwise omitted from the original papers mentioned above. One of the fundamental ideas in science is the ability to reproduce experiments and obtain the same results. Verification of the implementation of the Kurganov-Tadmor scheme instills confidence in its effectiveness in solving the one dimensional black-oil model.

1.2 Literature Review

The black-oil equations model the multi-phase multi-component flow of fluids in porous media. We consider the three component (oil, gas, and water), three phase (liquid, vapor, and aqua) model according to Tragenstein and Bell [19]. The black-oil model is popular in reservoir simulation because it incorporates the mass transfer and compressibility effects arising from phase transitions (Transgenstein and Bell [19]). Phases might disappear and reappear under extreme pressure conditions. Oil can be present in liquid or vapor form , gas can be present in all three phases and water is present only in the aqua phase if temperature changes are neglected. When all three phases are present, the black-oil model is saturated; otherwise, it is undersaturated. In this thesis, the saturated black-oil model is considered.

Analytic solutions to the black-oil equations do not exist, and this necessitates numerical solutions to the equations. However, finding numerical solutions is non-trivial and computationally demanding. On one hand, the mass conservation equation is strongly nonlinear and solutions to the black-oil equations can be discontinuous resulting in a numerically complex system of equations. On the other hand, large amounts of computational power are required because of the number of grid points needed for accuracy and the long run-times for simulations.

A significant step in the formulation of numerical algorithms for black-oil equations was achieved by Trangenstein and Bell in 1989 [19]. Since the black-oil model consists of a system of coupled equations whose solutions exhibit parabolic and hyperbolic characteristics, the system is decoupled into its parabolic and hyperbolic parts [19]. Taking advantage of this decoupling feature, sequential numerical algorithms which allow for the parabolic equation to be solved first and its solution to be used in the hyperbolic equation can be developed. The numerical algorithm used in this thesis follows this sequential structure.

The pressure and phase velocity are components of a parabolic equation which is relatively straightforward to solve, while the conservation of mass for the fluid components is hyperbolic in nature and poses the greatest challenge to researchers. The hyperbolic equation is strongly nonlinear, non-convex and is mathematically degenerate (Karimi et al. [8]). When the black-oil model is undersaturated, all the components (oil, gas, and water) might be present, but one of the phases might van-

ish. Mathematically, this leads to a degenerate set of equations which are nontrivial to solve.

Numerical solutions to the mass conservation equation are best obtained using high order and high resolution schemes that can accurately capture discontinuities in the solutions. The usual choice is Godunov schemes which approximate the solution with a piecewise constant or linear reconstruction of the solution variables. Pioneering work towards Godunov schemes was by Godunov in 1959 [6]. Although his original method was first order, higher order methods applicable to hyperbolic conservation laws have since been developed (e.g. Bell and Shubin [3], Bell et al. [2], and Harten et al. [7]). High-resolution Godunov methods have been applied to the black-oil model (e.g. Transgenstein and Bell [19] and Karimi et al. [8]). Godunov-type schemes are computationally expensive because they require the computation of local Riemann problems and complete computations of eigenstructures associated with the hyperbolic problem. Central schemes are a less computationally expensive alternative to Godunov schemes.

Finite volume central schemes do not require the computation of eigenstructures or solutions to local Riemann problems. The works of Lax and Friedrichs [12] pioneered the development of central schemes. The major disadvantage of central schemes is the large amount of numerical viscosity present when solving hyperbolic conservation laws (Leveque [13]). Numerical viscosity is an unwanted consequence of the discrete approximation and leads to smeared numerical solutions. Naderan et al. [17] show that

Lax-Friedrichs schemes are not suitable for numerically solving the black-oil problem whilst schemes such as the Nessyahu-Tadmor scheme (Nessyahu and Tadmor[18]) with less numerical viscosity are more suitable. However, when applied to the black-oil model, the numerical solution given by the Nessyahu-Tadmor scheme, whilst less diffusive than the Lax-Friedrichs solution, still has a large dependency on Courant-Friedrichs-Lewy (CFL) numbers (Naderan et al. [17]). At low CFL numbers, the discontinuities in the solution are not accurately resolved.

A family of central schemes introduced by Kurganov and Tadmor [11] does not depend on eigenstructures or CFL numbers and is Riemann-solver-free. These central schemes are a modification of the Nessyahu-Tadmor scheme with the major difference being the addition of maximal local speeds of propagation in the Kurganov-Tadmor schemes. The one dimensional Kurganov-Tadmor semi-discrete scheme exhibits less numerical viscosity than the Nessyahu-Tadmor scheme. In their paper, Kurganov and Tadmor [11] show that the Kurganov-Tadmor scheme applied to a number of hyperbolic conservation law equations is of higher resolution than the Nessyahu-Tadmor scheme. Compared to the Kurganov- Tadmor scheme, other schemes of higher order (e.g. Liu et al. [15], Kurganov and Levy [10]) and higher resolution (e.g. Lin [14]) have been developed. It is the focus of this thesis to strengthen the application of the second order semi-discrete Kurganov-Tadmor scheme to the black-oil model.

In their application of the Kurganov and Tadmor scheme to the black-oil problem, Naderan et al. [17] show both its suitability and ease of implementation. A

comparison between the Kurganov-Tadmor scheme and a high order Godunov-type scheme by Karimi et al. [8] further shows that the two schemes are of comparable accuracy when implemented on one-dimensional black-oil problems. However, the high order Godunov scheme is more accurate because of the computation of exact eigenstructures. The Kurganov-Tadmor scheme can still be preferred when the priority is ease of formulation and implementation whilst maintaining comparable accuracy to Godunov-type schemes (Karimi et al. [8]). This thesis applies the semi-discrete Kurganov-Tadmor scheme to the black-oil model to verify and extend the work of Karimi et al. [8]. Theoretical results on convergence of the Kurganov-Tadmor scheme do not currently exist ([9], [16]) and therefore it necessary to include numerical convergence rates in this work.

1.3 Thesis Outline

The setup for this thesis is as follows: Chapter 2 introduces the method of finite volumes in one dimension and explains its relevance to hyperbolic conservation laws. A formulation for the semi-discrete Kurganov-Tadmor scheme is also given. To confirm the order of convergence for the Kurganov-Tadmor scheme, we apply it to well-known model hyperbolic conservation laws (the advection equation and the inviscid Burgers equation) for which exact solutions can be computed. Numerical results and their discussion conclude the chapter.

In chapter 3 the mathematical model for the black-oil problem is introduced.

Variables and assumptions in the model are stated and a derivation of the pressure equation is provided. The pressure and mass component equations that compose the black-oil model are then discretized and the numerical implementation is given. Chapter 4 gives the validation for the application of the Kurganov-Tadmor scheme to the black-oil model through reproduced numerical results. Numerical solutions to the saturated black-oil model test case adapted from Transgenstein and Bell [19] are generated using the KT scheme and results are presented for comparison with works from Transgenstein and Bell [19] and Karimi et al. [8]. In addition, results to verify our simulation through small modifications to our main saturated black-oil test case are provided. Finally, chapter 5 is the conclusion for this thesis and presents future work.

Chapter 2

Finite Volume Methods for Hyperbolic Conservation Laws

Finite volume methods are well suited for conservation laws because the partial differential equation is discretized directly and solved over discrete control volumes which preserves the flux through the control volumes. This chapter introduces the fundamental concepts of the finite volume method for conservation laws in one dimension. Details of the Kurganov-Tadmor (KT) scheme are provided and the second order convergence of the KT scheme is verified by applying the scheme to conservation laws that can be solved explicitly.

2.1 Finite volume method

Consider the general form of a hyperbolic conservation law in one dimension:

$$u_t(x,t) + (f(u(x,t)))_x = 0, \qquad a < x < b, \quad t > 0. \tag{2.1}$$

Equation (2.1) can be written in a quasi-linear form:

$$u_t(x,t) + f'(u)u_x = 0. \tag{2.2}$$

The function $f(u)$ is the flux function. For the one dimensional case we also note that if $f'(u)$ is a constant then we have a linear hyperbolic equation. The advection equation, a linear hyperbolic equation is explored in section 2.3.2.

2.1.1 Implementation

We discretize in space only. A partition of the interval $[a, b]$ into cells $[x_{i-1/2}, x_{i+1/2}]$ of length (control volume) Δx is considered. For each cell, we pick the midpoint and denote it x_i, where i is from 1 to N.

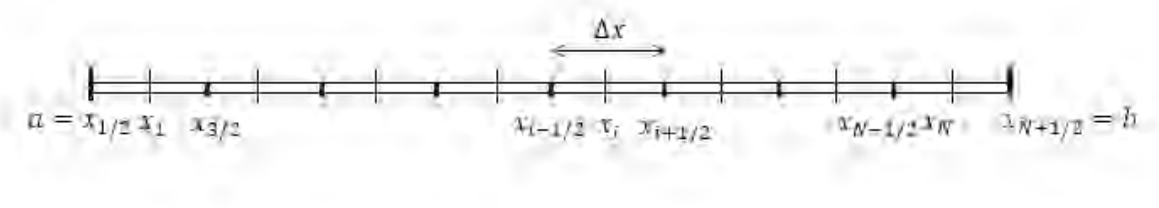

Figure 2.1 : Spatial discretization

The unknowns in the finite volume method approximate the average of the solution over the grid cell. Let U_i^n denote the approximation of the average $\bar{u}(x, t_n)$ over the ith interval at time t_n i.e.

$$U_i^n \approx \bar{u}(x_i, t_n) = \frac{1}{\Delta x} \int_{x_{i-1/2}}^{x_{i+1/2}} u(x, t_n) dx.$$

To derive equations of the scheme, we integrate equation (2.1) over the control volume and divide by Δx:

$$\frac{d}{dt}\left(\frac{1}{\Delta x} \int_{x_{i-1/2}}^{x_{i+1/2}} u(x, t) dx\right) + \frac{1}{\Delta x} \int_{x_{i-1/2}}^{x_{i+1/2}} (f(u(x, t))_x dx = 0,$$

which can be written as

$$\frac{d}{dt}\bar{u}(x_i,t) = (f(u(x_{i-1/2},t) - f(u(x_{i+1/2},t)). \tag{2.3}$$

Equation (2.3) is an ordinary differential equation (ODE) which can be solved by implicit or explicit time-marching algorithms. In this thesis, we use the forward Euler method to solve the ODE. Given U_i^n the cell average at time t_n, we want to approximate U_i^{n+1} the cell average at time t_{n+1} after a time interval of length $\Delta t = t_{n+1} - t_n$.

Applying forward Euler to equation (2.3) gives the numerical scheme:

$$U_i^{n+1} = U_i^n - \frac{\Delta t}{\Delta x}[f_{i+1/2}^n - f_{i-1/2}^n], \tag{2.4}$$

where the numerical flux $f_{i-1/2}^n$ and $f_{i+1/2}^n$ is determined for each finite volume scheme.

2.2 KT central scheme

2.2.1 Background

In a broad sense, central schemes are numerical methods for which an approximation to U_i at time step t^{n+1} is derived from a formulation that involves information from neighboring approximations for example U_{i-1} and U_{i+1} at time t^n. Central schemes usually only involve the computation of the numerical flux and do not require the evaluation of local Riemann problems [13],[11], which are costly to compute for nonlinear systems. Central schemes incorporate flux evaluations and in some cases evaluations

of the Jacobian of the flux, however because they are independent of complete eigenstructures of the PDE, they still lead to less computationally expensive solutions [11]. The major drawback of central schemes is the tendency to exhibit large amounts of numerical dissipation. These numerical effects affect the solutions to nonlinear conservation laws that have shocks and other discontinuities.

Pioneering work for central schemes was by Lax and Friedrichs. However, because the Lax-Friedrichs methods is first order, it requires fine grids and this results in a formulation that is expensive as solving Riemann problems [13]. In addition, the Lax-Friedrichs scheme is very dissipative and not suitable for most nonlinear conservation laws. A class of high resolution and high order central schemes, were presented by Nessyahu and Tadmor in 1990 [18]. For one dimensional problems the second order schemes by Nessyahu and Tadmor have numerical viscosity on the order of $\mathcal{O}((\Delta x)^4/\Delta t)$ [11]. At small time steps these schemes still lead to large amounts of numerical dissipation. As a refinement of the central schemes by Nessyahu and Tadmor, Kurganov and Tadmor introduced a family of central schemes that have numerical viscosity on the order of $\mathcal{O}((\Delta x)^3)$ for second order methods [11]. This smaller numerical viscosity and the independence from Δt, while maintaining a Riemann solver-free approach makes KT schemes good candidates to apply to conservation laws. In this paper we focus on the semi-discrete version of the Kurganov-Tadmor scheme presented in the next section.

2.2.2 Semi-discrete KT scheme

We use the same discretization as in section 2.1.1 and recall the general scheme:

$$U_i^{n+1} = U_i^n - \frac{\Delta t}{\Delta x}[f_{i+1/2}^n - f_{i-1/2}^n].$$

The numerical flux according to the Kurganov-Tadmor scheme is defined as follows:

$$f_{i+1/2}^n = \frac{1}{2}[f_{i+1/2}^+ + f_{i+1/2}^-] - \frac{1}{2}a_{i+1/2}(U_{i+1/2}^+ - U_{i+1/2}^-),$$

where

$$U_{i+1/2}^+ = U_{i+1} - \frac{\Delta x}{2}U_{x,i+1},$$

and

$$U_{i+1/2}^- = U_i + \frac{\Delta x}{2}U_{x,i}$$

are the right and left states respectively. The right and left intermediate fluxes are given by

$$f_{i+1/2}^+ = f(U_{i+1/2}^+),$$

and

$$f_{i+1/2}^- = f(U_{i+1/2}^-)$$

respectively. To reduce the oscillatory nature of central schemes, the approximate derivatives are defined by:

$$U_{x,i} = minmod\left(\frac{U_{i+1} - U_i}{\Delta x}, \frac{U_i - U_{i-1}}{\Delta x}\right),$$

$$U_{x,i+1} = minmod\left(\frac{U_{i+2} - U_{i+1}}{\Delta x}, \frac{U_{i+1} - U_i}{\Delta x}\right),$$

where the minmod function is a total-variation diminishing flux limiter given by

$$minmod(x,y) = \begin{cases} min(x,y) & x > 0 \text{ and } y > 0 \\ max(x,y) & x < 0 \text{ and } y < 0 \\ 0 & xy < 0 \end{cases}$$

The local wavespeed $a_{i+1/2}$ is the spectral radius of the Jacobian of the flux function defined by:

$$a_{i+1/2} = \rho(\frac{\partial f(\bar{u})}{\partial u}),$$

evaluated at

$$\bar{u}_i = \frac{1}{2}(U^+_{i+1/2} + U^-_{i+1/2}).$$

2.3 Rates of convergence for the KT scheme

In this section we apply the KT scheme to hyperbolic conservation laws for which we can determine exact solutions (ie. the advection equation and the inviscid Burger's equation). The goal is to numerically determine the order of convergence of the Kurganov-Tadmor scheme and the accuracy of solutions. In addition, this is a good first step in code development for our black oil problem which will be explored in chapters 3 and 4.

2.3.1 Norms for convergence

The L^∞ and L^1 norm are used in this thesis to evaluate convergence rates for the KT scheme. The L^∞ error is defined by

$$\|U(x,t^n) - u(x,t^n)\|_\infty = \max_{1\le i\le N} |U(x_i,t^n) - u(x_i,t^n)|,$$

while the L^1 error is defined by

$$\|U(x,t^n) - u(x,t^n)\|_1 = \Delta x \sum_{i=1}^{N} |U(x_i,t^n) - u(x_i,t^n)|.$$

2.3.2 Advection equation

The linear advection equation is a hyperbolic partial differential equation of the form

$$\frac{\partial u}{\partial t} + v\frac{\partial u}{\partial x} = 0. \tag{2.5}$$

The advection equation arises in transport processes. The function $u(x,t)$ represents for example the concentration or density of a substance that is advected by a one dimensional flow field whose local velocity is given by v. Here the flux is defined by

$$f(u) = vu.$$

The analytic solution to the advection equation is

$$u(x,t) = \bar{u}(x - vt)$$

for any initial function $\bar{u}(x)$. Physically, the profile of the solution is simply shifted to the left or to the right depending on the sign of v, corresponding to advection forward or advection backwards.

2.3.2.1 Numerical results

We solve the following advection equation on interval $[0, 1]$

$$u_t + u_x = 0, \tag{2.6}$$

with the following initial conditions:

$$u(x, 0) = \sin(x).$$

The boundary conditions $u(0, t)$ and $u(1, t)$ are given by the exact solution to this problem:

$$u(x, t) = \sin(x - t)$$

The Kurganov-Tadmor scheme gives a good approximation to the exact solution as shown in figure (2.2) for results generated with $\Delta t = 10^{-5}$ and $\Delta x = 0.03125$.

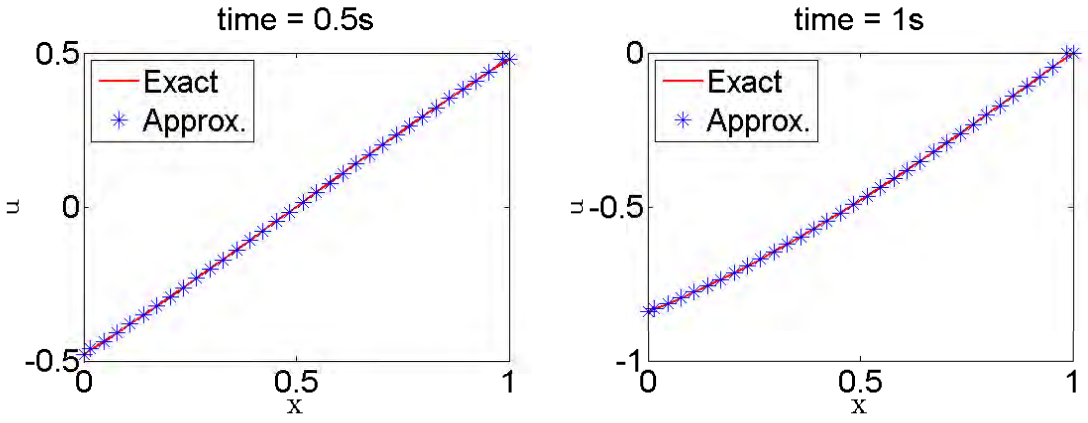

(a) (b)

Figure 2.2 : Solution $u(x, t) = \sin(x - t)$ at (a) $0.5s$ and (b) $1s$

With respect to the L^∞ norm, the KT scheme appears to be first order as shown in table (2.1) and in the L^1 norm, the KT scheme is approximately second order.

N	Δx	L^∞ error	Rate	L^1 error	Rate
4	$\frac{1}{4}$	7.441996e-2		3.550353e-2	
8	$\frac{1}{8}$	4.695229e-2	0.6644942	1.094080e-2	1.698244
16	$\frac{1}{16}$	2.608817e-2	0.8477995	3.096778e-3	1.820879
32	$\frac{1}{32}$	1.372245e-2	0.9268580	8.164255e-4	1.923375
64	$\frac{1}{64}$	7.050793e-3	0.9606805	2.064276e-4	1.983686

Table 2.1 : Rates of convergence in L^∞ and L^1 norm : $u(x,t) = \sin(x-t)$.

2.3.3 Inviscid Burger's equation

The inviscid Burgers equation is a nonlinear hyperbolic equation of the form

$$u_t + \left(\frac{u^2}{2}\right)_x = 0. \tag{2.7}$$

Many researchers use the inviscid Burgers equation in theoretical analysis of complicated nonlinear hyperbolic equations or in validating accuracy of numerical methods. The analytic solution for the inviscid Burgers equation can be obtained using the method of characteristics for sufficiently smooth initial data. For an initial function $g(x)$, the solution at some time t is defined implicitly by

$$u(x,t) = g(x - ut).$$

If the characteristics to the initial value problem cross, there is no classical solution to the inviscid Burgers equation.

2.3.3.1 Numerical Results

We solve the inviscid Burgers equation (2.7) on interval $[0, 1]$ subject to the following initial conditions

$$u_0(x) = u(x, 0) = x.$$

The boundary conditions $u(0, t)$ and $u(1, t)$ are given by the exact solution defined by:

$$u(x, t) = \frac{x}{1 + t}.$$

Figure (2.3) shows the exact and approximate curves for the solution using $\Delta x = 0.03125$ and $\Delta t = 10^{-5}$.

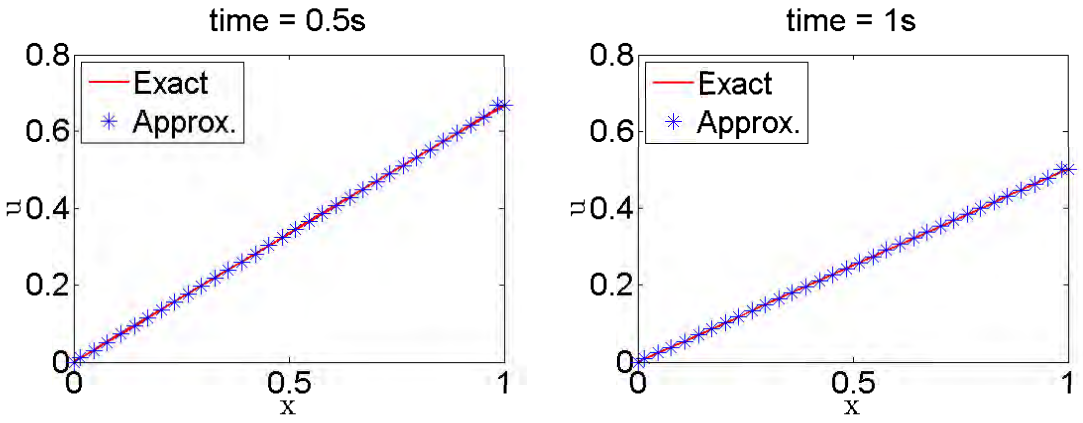

(a) (b)

Figure 2.3 : Solution $u(x, t) = \frac{x}{1+t}$ at (a) $0.5s$ and (b) $1s$

N	Δx	L^∞ error	Rate	L^1 error	Rate
4	$\frac{1}{4}$	5.517226e-2		2.006755e-2	
8	$\frac{1}{8}$	3.476626e-2	0.6658405	6.529612-3	1.619795
16	$\frac{1}{16}$	1.666105e-2	1.061623	1.588948e-3	2.038925
32	$\frac{1}{32}$	8.06717e-3	1.047142	3.894908e-4	2.028411
64	$\frac{1}{64}$	3.966517e-3	1.023393	9.699584e-5	2.005594

Table 2.2 : Rates of convergence in L^∞ and L^1 norm : $u(x,t) = \frac{x}{1+t}$.

The rates of convergence using a time step of $\Delta t = 10^{-5}$ for the L^∞ and L^1 norms are shown in table (2.2).

The KT scheme is presented as a second order scheme in [11]. However, from our tests on the advection and inviscid Burgers equations, the KT scheme exhibits a rate of convergence of approximately one in the L^∞ norm and a rate of convergence of approximately two in the L^1 norm. To determine the order of convergence, a theoretical analysis can also be done in terms of the truncation error for the KT scheme. Since the L^1 error is most widely accepted for conservation laws, we treat the KT scheme as approximately second order. In chapters 3 and 4 we apply the KT scheme to the black oil system of equations and present numerical results.

Chapter 3

Black-oil Model

The black-oil model is a means of calculating the phase behavior in a reservoir model. The phase behavior is characterized by defining the number of phases, phase amounts, phase compositions, and phase properties (molecular weight, density, and viscosity). It is also essential in reservoir simulation to know the derivatives of all phase properties with respect to pressure and composition. Trangenstein and Bell [19] provide and analyze the mathematical structure of the black-oil flow equations which consist of a parabolic and hyperbolic equation. The parabolic part contains pressure and velocity components of the flow as primitive variables and the hyperbolic part describes the conservation of mass for the fluid components. We first introduce the variables used in the black-oil equations according to Transgenstein and Bell [19].

3.1 Variable description

The components of the black-oil model are oil, gas, and water denoted by subscripts o, g, and w respectively. The components are found in different phases liquid, vapor, and aqua denoted by subscripts l, v, and a respectively. In the absence of capillary effects, all phases have the same pressure p. The vector $\mathbf{z} = \{z_o, z_g, z_w\}^T$ represents the mass components per pore volume whilst the volume of each phase per pore

volume is denoted by the vector $\mathbf{u} = \{u_l, u_v, u_a\}^T$. The fractions of the total fluid volume occupied by each of the three phases are the saturations

$$\mathbf{s} = \frac{\mathbf{u}}{\mathbf{e}^T\mathbf{u}},$$

where $\mathbf{e} = \{1, 1, 1\}^T$.

The phase velocities for the different phases $j = l, v, a$ are determined by Darcy's law

$$v_j = -\lambda_j(\frac{\partial p}{\partial x}),$$

where the mobility of phase j is defined as

$$\lambda_j = \frac{Kk_{r_j}}{\mu_j},$$

with K the rock permeability, k_{r_j} the relative permeability, and μ_j the dynamic viscosity. The vector of velocities is given by

$$\mathbf{v} = \{v_l, v_v, v_a\}^T.$$

Defining the total mobility as

$$\lambda = \sum_{j=l,v,a} \lambda_j,$$

the fractional flow is given by

$$f_j = \lambda_j/\lambda.$$

The total velocity can then be written as

$$v_t = \mathbf{v}^T\mathbf{e} = \lambda(\frac{\partial p}{\partial x}),$$

and

$$v_j = f_j v_t.$$

The volume formation factor matrix defined as

$$\mathbf{B} = \begin{bmatrix} B_l & 0 & 0 \\ 0 & B_v & 0 \\ 0 & 0 & B_a \end{bmatrix},$$

represents the ratio of the volume of each phase at reservoir condition to the volume of the same phase at stock tank condition. Neglecting thermal effects, the B_j's are functions of the pressure only. The solution ratio matrix $\mathbf{R}$ determines the distribution of each of the components in different phases. At stock tank conditions the components oil, gas, and water are primarily in liquid, vapor, and aqueous phases respectively; they are the principal components in those phases. The fraction of component i in phase j is given by R_{ij} where $i = o, g, w$ and $j = l, v, a$. The solution matrix is defined as the following:

$$\mathbf{R} = \begin{bmatrix} 1 & R_v & 0 \\ R_l & 1 & R_a \\ 0 & 0 & 1 \end{bmatrix}$$

where the solution ratios R_j are

$$R_l = \frac{z_{gl}}{z_{ol}}, R_v = \frac{z_{ov}}{z_{gv}}, \text{and } R_a = \frac{z_{ga}}{z_{wa}},$$

and z_{ij} is the mass component i in phase j per pore volume. The $R'_j s$ depend on the pressure. The volume of each phase per pore volume $\mathbf{u}$ can be written as a function of $\mathbf{z}$:

$$\mathbf{u} = \mathbf{BTz}, \tag{3.1}$$

where $\mathbf{T} = \mathbf{R}^{-1}$.

3.2 Black-oil equations

3.2.1 Mass conservation equation

Suppose the reservoir is an isolated system (ie, there is no interaction with the surrounding environment), then the mass of each component in the reservoir is conserved. The conservation of mass equation for the black-oil model is represented by:

$$\frac{\partial(\phi \mathbf{z})}{\partial t} + \frac{\partial}{\partial x}(\mathbf{RB^{-1}v}) = 0, \tag{3.2}$$

where ϕ is the pressure dependent porosity.

3.2.2 Pressure equation derivation

The equation of state states that the sum of the phase volumes is equal to the pore volume,

$$\mathbf{e^T u} = \mathbf{1} \tag{3.3}$$

that is,

$$u_l + u_v + u_a = 1.$$

Given the pressure p and the fluid composition $\mathbf{z}$ at a current time t we want to predict the value of the pressure at an advanced time $t + \Delta t$. A linearization of the equation of state results in the pressure equation for the black-oil system.

Let $\hat{\mathbf{u}}(t) = \mathbf{u}(p(t), \mathbf{z}(t))$. By Taylor's theorem, for each phase volume u_j, $j = l, v, a$, we have:

$$\begin{aligned}\hat{u_j}(t + \Delta t) - \hat{u_j}(t) &= u_j(p(t + \Delta t), \mathbf{z}(t + \Delta t)) - u_j(\mathbf{p}(t), \mathbf{z}(t)) \\ &= \Delta t \left(\frac{\partial u_j}{\partial p} \frac{\partial p}{\partial t} + \frac{\partial u_j}{\partial \mathbf{z}} \frac{\partial \mathbf{z}}{\partial t} \right) + O((\Delta t)^2).\end{aligned}$$

Therefore,

$$\frac{\hat{u_j}(t + \Delta t) - \hat{u_j}(t)}{\Delta t} = \left(\frac{\partial u_j}{\partial p} \frac{\partial p}{\partial t} + \frac{\partial u_j}{\partial \mathbf{z}} \frac{\partial \mathbf{z}}{\partial t} \right) + O(\Delta t).$$

After summing over the u_j's and dropping the $O(\Delta t)$,

$$\frac{\mathbf{e}^T(\hat{\mathbf{u}}(t + \Delta t) - \hat{\mathbf{u}}(t))}{\Delta t} \approx \mathbf{e}^T \left(\frac{\partial \mathbf{u}}{\partial p} \frac{\partial p}{\partial t} + \frac{\partial \mathbf{u}}{\partial \mathbf{z}} \frac{\partial \mathbf{z}}{\partial t} \right). \tag{3.4}$$

To satisfy the equation of state, we should have $\mathbf{e}^T \hat{\mathbf{u}}(t + \Delta t) = 1$, but it is not necessarily true that $\mathbf{e}^T \hat{\mathbf{u}}(t) = 1$. Thus the pressure is chosen to correct any existing volume discrepancy errors. Multiplying equation (3.4) by $(-\phi)$ gives,

$$-\phi \left(\frac{1 - \mathbf{e}^T \mathbf{u}}{\Delta t} \right) = -\phi \left(\mathbf{e}^T \frac{\partial \mathbf{u}}{\partial p} \frac{\partial p}{\partial t} + \mathbf{e}^T \frac{\partial \mathbf{u}}{\partial \mathbf{z}} \frac{\partial \mathbf{z}}{\partial t} \right),$$

which simplifies to

$$\frac{\mathbf{e}^T \mathbf{u} - 1}{\Delta t} \phi = -\phi \left(\mathbf{e}^T \frac{\partial \mathbf{u}}{\partial p} \frac{\partial p}{\partial t} + \mathbf{e}^T \frac{\partial \mathbf{u}}{\partial \mathbf{z}} \frac{\partial \mathbf{z}}{\partial t} \right). \tag{3.5}$$

An expression for $\frac{\partial \mathbf{z}}{\partial t}$ can be obtained by considering the mass conservation equation (3.2). Note that

$$\frac{\partial(\phi \mathbf{z})}{\partial t} = \mathbf{z}\frac{\partial \phi}{\partial t} + \phi\frac{\partial \mathbf{z}}{\partial t}$$
$$\frac{\partial(\phi \mathbf{z})}{\partial t} = -\frac{\partial}{\partial x}(\mathbf{R}\mathbf{B}^{-1}\mathbf{v}).$$

Solving for $\frac{\partial \mathbf{z}}{\partial t}$, we find

$$\frac{\partial \mathbf{z}}{\partial t} = -\frac{1}{\phi}\left(\mathbf{z}\frac{\partial \phi}{\partial t} + \frac{\partial}{\partial x}(\mathbf{R}\mathbf{B}^{-1}\mathbf{v})\right).$$

The right-hand side of equation (3.5) can be written as

$$\begin{aligned} -\phi\left(\mathbf{e}^T\frac{\partial \mathbf{u}}{\partial p}\frac{\partial p}{\partial t} + \mathbf{e}^T\frac{\partial \mathbf{u}}{\partial \mathbf{z}}\frac{\partial \mathbf{z}}{\partial t}\right) &= -\phi\mathbf{e}^T\frac{\partial \mathbf{u}}{\partial p}\frac{\partial p}{\partial t} + \mathbf{e}^T\frac{\partial \mathbf{u}}{\partial \mathbf{z}}\left(\mathbf{z}\frac{\partial \phi}{\partial t} + \frac{\partial}{\partial x}(\mathbf{R}\mathbf{B}^{-1}\mathbf{v})\right) \\ &= \left(-\phi\mathbf{e}^T\frac{\partial \mathbf{u}}{\partial p} + \mathbf{e}^T\frac{\partial \mathbf{u}}{\partial \mathbf{z}}\mathbf{z}\frac{\partial \phi}{\partial p}\right)\frac{\partial p}{\partial t} + \mathbf{e}^T\frac{\partial \mathbf{u}}{\partial \mathbf{z}}\frac{\partial}{\partial x}(\mathbf{R}\mathbf{B}^{-1}\mathbf{v}). \end{aligned}$$

Putting everything together in equation (3.5), we get the pressure equation

$$\phi\left(\frac{\mathbf{e}^T\mathbf{u} - 1}{\Delta t}\right) = \left(-\phi\mathbf{e}^T\frac{\partial \mathbf{u}}{\partial p} + \mathbf{e}^T\frac{\partial \mathbf{u}}{\partial \mathbf{z}}\mathbf{z}\frac{\partial \phi}{\partial p}\right)\frac{\partial p}{\partial t} + \mathbf{e}^T\frac{\partial \mathbf{u}}{\partial \mathbf{z}}\frac{\partial}{\partial x}(\mathbf{R}\mathbf{B}^{-1}\mathbf{v}). \tag{3.6}$$

3.2.3 System of governing equations

The black-oil standard phase model that we consider in this thesis is given by the system of equation (3.2) and equation (3.6) over the interval $[0, L]$:

$$\left(-\phi \mathbf{e}^T \frac{\partial \mathbf{u}}{\partial p} + \mathbf{e}^T \mathbf{u} \frac{\partial \phi}{\partial p} \right) \frac{\partial p}{\partial t} + \mathbf{e}^T \frac{\partial \mathbf{u}}{\partial \mathbf{z}} \frac{\partial}{\partial x} (\mathbf{R}\mathbf{B}^{-\mathbf{1}}\mathbf{v}) = \frac{\mathbf{e}^T \mathbf{u} - 1}{\Delta t} \phi, \tag{3.7}$$

$$\frac{\partial (\phi \mathbf{z})}{\partial t} + \frac{\partial}{\partial x} (\mathbf{R}\mathbf{B}^{-\mathbf{1}}\mathbf{v}) = 0, \tag{3.8}$$

given initial and boundary conditions :

$p(x, t = 0) = p_{IC}$,

$\mathbf{z}(x, t = 0) = \mathbf{z}_{IC}$,

$p(x = 0, t) = p_{BC,0}$,

$p(x = L, t) = p_{BC,L}$,

$\mathbf{z}(x = 0, t) = \mathbf{z}_{BC,0}$.

3.3 Numerical method

The finite volume method is used to discretize equations (3.7) and (3.8). For a domain of length L, we consider an evenly spaced grid of N intervals. Let the control volume C_i be the interval $(x_{i-1/2}, x_{i+1/2})$ of length

$$\Delta x = \frac{L}{N},$$

for $1 \leq i \leq N$. The nodal points x_i for $1 \leq i \leq N$ are the midpoints of the intervals C_i.

3.3.1 Numerical pressure equation derivation

For simplicity in equation (3.7), we define

$$\alpha(p, \mathbf{z}) = -\phi \mathbf{e}^T \frac{\partial \mathbf{u}}{\partial p} + \mathbf{e}^T \mathbf{u} \frac{\partial \phi}{\partial p},$$

and

$$\beta(p, \mathbf{z}) = \frac{\mathbf{e}^T \mathbf{u} - 1}{\Delta t} \phi.$$

Integrating equation (3.7) over C_i results in the following expression

$$\int_{C_i} \alpha \frac{\partial p}{\partial t} dx + \int_{C_i} \mathbf{e}^T \mathbf{B} \mathbf{T} \frac{\partial}{\partial x} (\mathbf{R} \mathbf{B}^{-1} \mathbf{v}) dx = \int_{C_i} \beta dx. \tag{3.9}$$

By assuming the pressure is constant over the control volume, $\mathbf{R}\mathbf{B}^{-1}$ is independent of x. Equation (3.9) then becomes

$$\int_{C_i} \alpha \frac{\partial p}{\partial t} dx + \int_{C_i} \mathbf{e}^T \mathbf{B} \mathbf{T} \mathbf{R} \mathbf{B}^{-1} \frac{\partial}{\partial x} \mathbf{v} dx = \int_{C_i} \beta dx,$$

which simplifies to

$$\int_{C_i} \alpha \frac{\partial p}{\partial t} dx + \int_{C_i} \frac{\partial (\mathbf{e}^T \mathbf{v})}{\partial x} dx = \int_{C_i} \beta dx,$$

and since $\mathbf{v}_t = \mathbf{e}^T \mathbf{v}$ we have the following

$$\int_{C_i} \alpha \frac{\partial p}{\partial t} dx + \int_{C_i} \frac{\partial \mathbf{v}_t}{\partial x} dx = \int_{C_i} \beta dx.$$

An approximation of $\frac{\partial p}{\partial t}$ using finite differences gives

$$\int_{x_{i-1/2}}^{x_{i+1/2}} \alpha(p, \mathbf{z}) \frac{p^{n+1} - p^n}{\Delta t} dx + \int_{x_{i-1/2}}^{x_{i+1/2}} \frac{\partial \mathbf{v}_t}{\partial x} dx = \int_{x_{i-1/2}}^{x_{i+1/2}} \beta(p, \mathbf{z}) dx, \tag{3.10}$$

for all $1 \leq i \leq N$.

Let p_i^n be the numerical pressure in C_i at t^n and $\mathbf{z}_i^n$ be the numerical component densities defined by

$$\mathbf{z}_i^n = \begin{pmatrix} z_{o,i}^n \\ z_{g,i}^n \\ z_{w,i}^n \end{pmatrix}.$$

Equation (3.10) yields

$$\alpha(p_i^n, \mathbf{z}_i^n)\frac{p_i^{n+1} - p_i^n}{\Delta t}\Delta x + v_t^{n+1}(x_{i+1/2}) - v_t^{n+1}(x_{i-1/2}) = \beta(p_i^n, \mathbf{z}_i^n)\Delta x,$$

where

$$v_t^{n+1}(x_{i+1/2}) = v_{t,i+1/2}^{n+1} = -\lambda_{i+1/2}\frac{p_{i+1}^{n+1} - p_i^{n+1}}{\Delta x}, \tag{3.11}$$

and $\lambda_{i+1/2}$ is the harmonic average of λ_i and λ_{i+1}:

$$\lambda_{i+1/2} = \frac{2\lambda_i\lambda_{i+1}}{\lambda_i + \lambda_{i+1}}. \tag{3.12}$$

The implicit equation for pressure for all $1 \leq i \leq N$ is therefore:

$$\alpha(p_i^n, \mathbf{z}_i^n)(p_i^{n+1} - p_i^n)\Delta x + \Delta t\left[-\lambda_{i+1/2}\frac{p_{i+1}^{n+1} - p_i^{n+1}}{\Delta x} + \lambda_{i-1/2}\frac{p_i^{n+1} - p_{i-1}^{n+1}}{\Delta x}\right] = \beta(p_i^n, \mathbf{z}_i^n)\Delta x\Delta t. \tag{3.13}$$

3.3.2 Linear system for pressure equation

We rewrite (3.13) as

$$-\frac{\Delta t}{\Delta x}\lambda_{i-1/2}p_{i-1}^{n+1} + \left(\alpha_i\Delta x + \frac{\Delta t}{\Delta x}\lambda_{i+1/2} + \frac{\Delta t}{\Delta x}\lambda_{i-1/2}\right)p_i^{n+1} - \lambda_{i+1/2}\frac{\Delta t}{\Delta x}p_{i+1}^{n+1} = \beta_i\Delta x\Delta t + \alpha_i p_i^n\Delta x \tag{3.14}$$

where,

$$\alpha_i = \alpha(p_i^n, \mathbf{z}_i^n) \qquad \text{and} \qquad \beta_i = \beta(p_i^n, \mathbf{z}_i^n).$$

Let $\mathbf{P}_{matrix}$ denote the pressure matrix which is an $N \times N$ matrix where N is the number of intervals as stated above. Let $\mathbf{b}_{rhs}$ denote the right-hand side of pressure equation. Then the linear system is given by

$$\mathbf{P}_{matrix}\vec{\mathbf{p}} = \mathbf{b}_{rhs}.$$

Initial and boundary conditions are provided for the system of equations (3.7) and (3.8). These conditions affect the first and last rows of the matrix as indicated below. The first row of the system ($i = 1$), can be written as

$$\begin{aligned}
\mathbf{P}_{matrix}(1,1) &= \alpha(p_1, \mathbf{z}_1)\Delta x + \frac{\Delta t}{\Delta x}\lambda_{3/2} + \frac{\Delta t}{\Delta x}\lambda_{1/2}, \\
\mathbf{P}_{matrix}(1,2) &= -\frac{\Delta t}{\Delta x}\lambda_{3/2}, \\
\mathbf{b}_{rhs}(1) &= \beta(p_1, \mathbf{z}_1)\Delta x \Delta t + \alpha(p_1, \mathbf{z}_1)p_1\Delta x + \lambda_{1/2}\frac{\Delta t}{\Delta x}p_{BC,0}.
\end{aligned}$$

For the rows ($2 \leq i \leq N-1$), we have

$$\begin{aligned}
\mathbf{P}_{matrix}(i, i-1) &= -\lambda_{i-1/2}\frac{\Delta t}{\Delta x}. \\
\mathbf{P}_{matrix}(i, i+1) &= -\lambda_{i+1/2}\frac{\Delta t}{\Delta x}, \\
\mathbf{P}_{matrix}(i, i) &= \alpha(p_i, \mathbf{z}_i)\Delta x + \lambda_{i+1/2}\frac{\Delta t}{\Delta x} + \lambda_{i-1/2}\frac{\Delta t}{\Delta x}, \\
\mathbf{b}_{rhs}(i) &= \beta(p_i, \mathbf{z}_i)\Delta x \Delta t + \alpha(p_i, \mathbf{z}_i)p_i\Delta x.
\end{aligned}$$

The last row ($i = N$) can be expressed as

$$\mathbf{P}_{matrix}(N,N) = \alpha(p_N, \mathbf{z}_N)\Delta x + \frac{\Delta t}{\Delta x}\lambda_{N+1/2} + \frac{\Delta t}{\Delta x}\lambda_{N-1/2},$$
$$\mathbf{P}_{matrix}(N,N-1) = -\lambda_{N-1/2}\frac{\Delta t}{\Delta x},$$
$$\mathbf{b}_{rhs}(N) = \beta(p_N, \mathbf{z}_N)\Delta x \Delta t + \alpha(p_N, \mathbf{z}_N)p_N \Delta x + \frac{\Delta t}{\Delta x}\lambda_{N+1/2}p_{BC,L}.$$

3.3.3 Pressure derivative expressions

We present expressions for some of the derivatives in the pressure equation.

By equation (3.1) and since $\mathbf{z}$ does not depend on pressure,

$$\frac{\partial \mathbf{u}}{\partial p} = \frac{\partial(\mathbf{BTz})}{\partial p} = \frac{\partial(\mathbf{BT})}{\partial p}\mathbf{z}.$$

Thus the following holds:

$$\frac{\partial(\mathbf{BT})}{\partial p} = \begin{pmatrix} \frac{\partial}{\partial p}\left(\frac{B_l}{1-R_lR_v}\right) & -\frac{\partial}{\partial p}\left(\frac{B_lR_v}{1-R_lR_v}\right) & \frac{\partial}{\partial p}\left(\frac{B_lR_aR_v}{1-R_lR_v}\right) \\ -\frac{\partial}{\partial p}\left(\frac{B_vR_l}{1-R_lR_v}\right) & \frac{\partial}{\partial p}\left(\frac{B_v}{1-R_lR_v}\right) & -\frac{\partial}{\partial p}\left(\frac{B_vR_a}{1-R_lR_v}\right) \\ 0 & 0 & \frac{\partial B_a}{\partial p} \end{pmatrix},$$

where

$$\frac{\partial}{\partial p}\left(\frac{B_l}{1-R_lR_v}\right) = \frac{1}{1-R_lR_v}\frac{\partial B_l}{\partial p} + B_l\frac{\partial}{\partial p}(1-R_lR_v)^{-1},$$

with,

$$\frac{\partial}{\partial p}(1-R_lR_v)^{-1} = -(1-R_lR_v)^{-2}\left[-R_v\frac{\partial R_l}{\partial p} - R_l\frac{\partial R_v}{\partial p}\right];$$

$$\frac{\partial}{\partial p}\left(\frac{B_lR_v}{1-R_lR_v}\right) = \frac{1}{1-R_lR_v}\left[B_l\frac{\partial R_v}{\partial p} + R_v\frac{\partial B_l}{\partial p}\right] + B_lR_v\frac{\partial}{\partial p}(1-R_lR_v)^{-1},$$

$$\frac{\partial}{\partial p}\left(\frac{B_l R_a R_v}{1-R_l R_v}\right) = \frac{1}{1-R_l R_v}\left[B_l\left(R_a\frac{\partial R_v}{\partial p}+R_v\frac{\partial R_a}{\partial p}\right)+R_a R_v\frac{\partial B_l}{\partial p}\right]+B_l R_a R_v\frac{\partial}{\partial p}(1-R_l R_v)^{-1},$$

$$\frac{\partial}{\partial p}\left(\frac{B_v R_l}{1-R_l R_v}\right) = \frac{1}{1-R_l R_v}\left[B_v\frac{\partial R_l}{\partial p}+R_l\frac{\partial B_v}{\partial p}\right]+B_v R_l\frac{\partial}{\partial p}(1-R_l R_v)^{-1},$$

$$\frac{\partial}{\partial p}\left(\frac{B_v}{1-R_l R_v}\right) = \frac{1}{1-R_l R_v}\frac{\partial B_v}{\partial p}+B_v\frac{\partial}{\partial p}(1-R_l R_v)^{-1},$$

and

$$\frac{\partial}{\partial p}\left(\frac{B_v R_a}{1-R_l R_v}\right) = \frac{1}{1-R_l R_v}\left[B_v\frac{\partial R_a}{\partial p}+R_a\frac{\partial B_v}{\partial p}\right]+B_v R_a\frac{\partial}{\partial p}(1-R_l R_v)^{-1}.$$

3.3.4 Mass component equation

To derive equations of the numerical scheme corresponding to equation (3.8), we integrate the PDE over the control volume:

$$\frac{d}{dt}\int_{C_i}\phi(p)\mathbf{z}(x,t)dx+\int_{C_i}\frac{d\mathbf{F}(\mathbf{z}(x,t))}{dx}dx=0,$$

where $\mathbf{F}=\mathbf{R}\mathbf{B}^{-1}\mathbf{v}$. This yields:

$$\frac{d}{dt}\int_{C_i}\phi(p)\mathbf{z}(x,t)dx=(\mathbf{F}(\mathbf{z}(x_{i-1/2},t)-\mathbf{F}(\mathbf{z}(x_{i+1/2},t)). \tag{3.15}$$

Equation (3.15) is an ordinary differential equation which we solve using the forward Euler method. Given $\mathbf{z}_i^n$ the cell average at time t_n, we want to approximate $\mathbf{z}_i^{n+1}$ the cell average at time t_{n+1} after a time interval of length $\Delta t=t_{n+1}-t_n$. We obtain:

$$\mathbf{z}_i^{n+1}=\mathbf{z}_i^n-\frac{\Delta t}{\phi(p_i^{n+1})\Delta x}[\hat{\mathbf{F}}_{i-1/2}-\hat{\mathbf{F}}_{i+1/2}] \tag{3.16}$$

where,

$$\mathbf{z}_i^n = \frac{1}{\Delta x}\int_{C_i} \mathbf{z}(x, t^n).$$

and $\hat{\mathbf{F}}_{i\pm1/2}$ is the numerical flux vector associated with the exact flux $\mathbf{F}_{i+1/2} = \mathbf{RB^{-1}v}$ evaluated at the interface $x_{i\pm1/2}$.

3.3.5 KT scheme implementation

Consider the scheme for solving the mass conservation equation:

$$\mathbf{z}_i^{n+1} - \mathbf{z}_i^n = -\frac{\Delta t}{\phi(p_i)\Delta x}[\hat{\mathbf{F}}_{i+1/2} - \hat{\mathbf{F}}_{i-1/2}]$$

The numerical flux according to the Kurganov-Tadmor scheme is as follows:

$$\hat{\mathbf{F}}_{i+1/2} = \frac{1}{2}[\mathbf{F}^+_{i+1/2} + \mathbf{F}^-_{i+1/2}] - \frac{1}{2}a_{i+1/2}(\mathbf{z}^+_{i+1/2} - \mathbf{z}^-_{i+1/2}), \tag{3.17}$$

where,

$$\mathbf{z}^+_{i+1/2} = \mathbf{z}_{i+1} - \frac{\Delta x}{2}\mathbf{z}_{x,i+1}$$

and

$$\mathbf{z}^-_{i+1/2} = \mathbf{z}_i + \frac{\Delta x}{2}\mathbf{z}_{x,i}$$

are the right and left states respectively. The intermediate fluxes are given by

$$\mathbf{F}^\pm_{i+1/2} = \mathbf{F}(\mathbf{z}^\pm_{i+1/2}).$$

The approximate derivatives are given by

$$\mathbf{z}_{x,i} = minmod\left(\frac{\mathbf{z}_{i+1} - \mathbf{z}_i}{\Delta x}, \frac{\mathbf{z}_i - \mathbf{z}_{i-1}}{\Delta x}\right)$$

where the minmod function is as defined in chapter 2. The local wavespeed $a_{i+1/2}$ is the Jacobian of the flux function defined as

$$a_{i+1/2} = \frac{\partial F(\bar{\mathbf{z}})}{\partial \mathbf{z}},$$

evaluated at $\bar{\mathbf{z}} = \frac{1}{2}(\mathbf{z}^+_{i+1/2} + \mathbf{z}^-_{i+1/2})$.

3.3.5.1 Derivative Expressions

In computing the wavespeed we require the partial derivative of $\mathbf{F} = \mathbf{RB^{-1}v}$ with respect to $\mathbf{z}$. Note that $\mathbf{R}$ and $\mathbf{B^{-1}}$ both do not depend on $\mathbf{z}$ thus

$$\frac{\partial \mathbf{F}}{\partial \mathbf{z}} = \frac{\partial(\mathbf{RB^{-1}v})}{\partial \mathbf{z}} = \mathbf{RB^{-1}}\frac{\partial \mathbf{v}}{\partial \mathbf{z}}$$

where

$$\mathbf{v} = -\frac{\partial p}{\partial x}\begin{pmatrix}\lambda_l \\ \lambda_v \\ \lambda_a\end{pmatrix} = -\frac{\partial p}{\partial x}K\begin{pmatrix}\frac{k_{rl}}{\mu_l} \\ \frac{k_{rv}}{\mu_v} \\ \frac{k_{ra}}{\mu_a}\end{pmatrix}$$

Therefore,

$$\frac{\partial \mathbf{F}}{\partial \mathbf{z}} = -K\frac{\partial p}{\partial x}\mathbf{RB^{-1}} = \begin{pmatrix} \frac{1}{\mu_l}\frac{\partial k_{rl}}{\partial z_o} & \frac{1}{\mu_l}\frac{\partial k_{rl}}{\partial z_g} & \frac{1}{\mu_l}\frac{\partial k_{rl}}{\partial z_w} \\ \frac{1}{\mu_v}\frac{\partial k_{rv}}{\partial z_o} & \frac{1}{\mu_v}\frac{\partial k_{rv}}{\partial z_g} & \frac{1}{\mu_v}\frac{\partial k_{rv}}{\partial z_w} \\ \frac{1}{\mu_a}\frac{\partial k_{ra}}{\partial z_o} & \frac{1}{\mu_a}\frac{\partial k_{ra}}{\partial z_g} & \frac{1}{\mu_a}\frac{\partial k_{ra}}{\partial z_w} \end{pmatrix}.$$

Let $j = o, g, w$. The expressions for the relative permeabilities $k'_{r_j}s$ are

$$k_{r_l}(\mathbf{z}, p) = (1 - s_v(\mathbf{z}, p) - s_a(\mathbf{z}, p))(1 - s_v(\mathbf{z}, p))(1 - s_a(\mathbf{z}, p)),$$

$$k_{r_v}(\mathbf{z}, p) = (s_v(\mathbf{z}, p))^2,$$

$$k_{r_a}(\mathbf{z}, p) = (s_a(\mathbf{z}, p))^2.$$

The derivatives are given by

$$\begin{aligned}\frac{\partial k_{r_l}}{\partial z_j} &= \frac{\partial}{\partial z_j}(1 - s_v^2 s_a - s_a^2 s_v + s_v^2 + s_a^2 + 3s_v s_a - 2s_v - 2s_a) \\ &= -\left(2s_v s_a \frac{\partial s_v}{\partial z_j} + s_v^2 \frac{\partial s_a}{\partial z_j}\right) - \left(2s_v s_a \frac{\partial s_a}{\partial z_j} + s_a^2 \frac{\partial s_v}{\partial z_j}\right) + 2s_v \frac{\partial s_v}{\partial z_j} + 2s_a \frac{\partial s_a}{\partial z_j} + \\ &+ 3s_v \frac{\partial s_a}{\partial z_j} + 3s_a \frac{\partial s_v}{\partial z_j} - 2\frac{\partial s_v}{\partial z_j} - 2\frac{\partial s_a}{\partial z_j},\end{aligned}$$

$$\frac{\partial k_{r_v}}{\partial z_j} = 2s_v \frac{\partial s_v}{\partial z_j} \qquad \text{and ,} \qquad \frac{\partial k_{r_a}}{\partial z_j} = 2s_a \frac{\partial s_a}{\partial z_j}$$

where

$$\begin{aligned}\frac{\partial s_v}{\partial z_j} = \frac{\partial}{\partial z_j}\left(\frac{u_v}{\mathbf{e}^T\mathbf{u}}\right) &= \frac{1}{\mathbf{e}^T\mathbf{u}}\frac{\partial u_v}{\partial z_j} - \frac{1}{(\mathbf{e}^T\mathbf{u})^2}\mathbf{e}^T(\mathbf{BTe}_j)u_v \\ &= \frac{\mathbf{e}_2^T(\mathbf{BTe}_j)}{\mathbf{e}^T\mathbf{u}} - \frac{1}{(\mathbf{e}^T\mathbf{u})^2}\mathbf{e}^T(\mathbf{BTe}_j)u_v,\end{aligned}$$

and

$$\begin{aligned}\frac{\partial s_a}{\partial z_j} = \frac{\partial}{\partial z_j}\left(\frac{u_v}{\mathbf{e}^T\mathbf{u}}\right) &= \frac{1}{\mathbf{e}^T\mathbf{u}}\frac{\partial u_a}{\partial z_j} - \frac{1}{(\mathbf{e}^T\mathbf{u})^2}\mathbf{e}^T(\mathbf{BTe}_j)u_a \\ &= \frac{\mathbf{e}_3^T(\mathbf{BTe}_j)}{\mathbf{e}^T\mathbf{u}} - \frac{1}{(\mathbf{e}^T\mathbf{u})^2}\mathbf{e}^T(\mathbf{BTe}_j)u_a.\end{aligned}$$

The vector $\mathbf{e}_j$ has a value of one for the j^{th} component and zero elsewhere.

3.3.5.2 Numerical Implementation

The scheme is based on a 5 point stencil, that is, the value at $\mathbf{z}_i$ depends on $\mathbf{z}_{i-2}, \mathbf{z}_{i-1}, \mathbf{z}_{i+1}$ and $\mathbf{z}_{i+2}$. We therefore consider the cases $\mathbf{z}_1, \mathbf{z}_2, \mathbf{z}_{N-1},$ and $\mathbf{z}_N$ separately because of their dependencies on boundary conditions and nodes that go beyond our discretization.

For $(i = 1)$, we have

$$\mathbf{z}_1^{n+1} - \mathbf{z}_1^n = -\frac{\Delta t}{\phi_1 \Delta x}[\hat{\mathbf{F}}_{3/2} - \hat{\mathbf{F}}_{1/2}],$$

where the right numerical flux is given by

$$\hat{\mathbf{F}}_{3/2} = \frac{1}{2}[\mathbf{F}^+_{3/2} + \mathbf{F}^-_{3/2}] - \frac{1}{2}a_{3/2}[\mathbf{z}^+_{3/2} - \mathbf{z}^-_{3/2}],$$

where the right and left states are

$$\mathbf{z}^+_{3/2} = \mathbf{z}_2 - \frac{\Delta x}{2}\mathbf{z}_{x,2},$$

and

$$\mathbf{z}^-_{3/2} = \mathbf{z}_1 + \frac{\Delta x}{2}\mathbf{z}_{x,1}$$

respectively. The approximate derivatives are given by,

$$\mathbf{z}_{x,2} = minmod\left(\frac{\mathbf{z}_3 - \mathbf{z}_2}{\Delta x}, \frac{\mathbf{z}_2 - \mathbf{z}_1}{\Delta x}\right),$$

and

$$\mathbf{z}_{x,1} = minmod\left(\frac{\mathbf{z}_2 - \mathbf{z}_1}{\Delta x}, \frac{\mathbf{z}_1 - \mathbf{z}_{BC,0}}{\Delta x}\right)$$

where

$$z_{BC,0} = \mathbf{z}(x = 0, t),$$

is the inflow boundary condition. The intermediate fluxes are given by

$$\mathbf{F}^{\pm}_{3/2} = \mathbf{F}(\mathbf{z}^{\pm}_{3/2}).$$

The left numerical flux is given by

$$\hat{\mathbf{F}}_{1/2} = \frac{1}{2}[\mathbf{F}^+_{1/2} + \mathbf{F}^-_{1/2}] - \frac{1}{2}a_{1/2}[\mathbf{z}^+_{1/2} - \mathbf{z}^-_{1/2}],$$

where the right and left states are

$$\mathbf{z}^{+}_{1/2} = \mathbf{z}_1 - \frac{\Delta x}{2}\mathbf{z}_{x,1},$$

and

$$\mathbf{z}^{-}_{1/2} = \mathbf{z}_{BC,0}$$

respectively. The intermediate fluxes are given by

$$\mathbf{F}^{\pm}_{1/2} = \mathbf{F}(\mathbf{z}^{\pm}_{1/2}).$$

We do not have a outflow boundary condition therefore $\mathbf{z}(L) = \mathbf{z}_N$. For (i = N) we have,

$$\mathbf{z}^{n+1}_N - \mathbf{z}^{n}_N = -\frac{\Delta t}{\phi_N \Delta x}[\hat{\mathbf{F}}_{N+1/2} - \hat{\mathbf{F}}_{N-1/2}],$$

where the right numerical flux is

$$\hat{\mathbf{F}}_{N+1/2} = \frac{1}{2}[\mathbf{F}^{+}_{N+1/2} + \mathbf{F}^{-}_{N+1/2}] - \frac{1}{2}a_{N+1/2}[\mathbf{z}^{+}_{N+1/2} - \mathbf{z}^{-}_{N+1/2}].$$

The right and left states are

$$\mathbf{z}^{+}_{N+1/2} = \mathbf{z}_N,$$

and

$$\mathbf{z}^{-}_{N+1/2} = \mathbf{z}_N + \frac{\Delta x}{2}\mathbf{z}_{x,N}$$

respectively where the approximate derivative

$$\mathbf{z}_{x,N} = \frac{\mathbf{z}_N - \mathbf{z}_{N-1}}{\Delta x}.$$

The intermediate fluxes are given by

$$\mathbf{F}^{\pm}_{N+1/2} = \mathbf{F}(\mathbf{z}^{\pm}_{N+1/2}).$$

The left numerical flux is given by

$$\hat{\mathbf{F}}_{N-1/2} = \frac{1}{2}[\mathbf{F}^{+}_{N-1/2} + \mathbf{F}^{-}_{N-1/2}] - \frac{1}{2}a_{N-1/2}[\mathbf{z}^{+}_{N-1/2} - \mathbf{z}^{-}_{N-1/2}],$$

where the right and left states are

$$\mathbf{z}^{+}_{N-1/2} = \mathbf{z}_N - \frac{\Delta x}{2}\mathbf{z}_{x,N},$$

and

$$\mathbf{z}^{-}_{N-1/2} = \mathbf{z}_{N-1} - \frac{\Delta x}{2}\mathbf{z}_{x,N-1}$$

respectively. The approximate derivative

$$\mathbf{z}_{x,N-1} = minmod\left(\frac{\mathbf{z}_N - \mathbf{z}_{N-1}}{\Delta x}, \frac{\mathbf{z}_{N-1} - \mathbf{z}_{N-2}}{\Delta x}\right).$$

The intermediate fluxes are given by $\mathbf{F}^{\pm}_{N-1/2} = \mathbf{F}(\mathbf{z}^{\pm}_{N-1/2})$.

In this chapter we have introduced the variables and equations that make up the black-oil model. Numerical formulations for both the pressure and the mass conservation equation have also been provided. In chapter 4 we present a test case adapted from Transgenstein and Bell and show numerical results for the implementation of the Kurganov-Tadmor scheme on the black-oil system of equations.

Chapter 4

Numerical Results

4.1 Saturated black-oil model

This test case for the saturated black-oil simulation originates from Trangenstein and Bell [19] and is further used in Naderan et. al [17] and Karimi et al. [8]. The initial reservoir pressure is 1800 psi whilst the injection and production pressures are at 2000 psi and 1600 psi respectively. Initial and injection component densities are given by

$$z_{IC} = \begin{pmatrix} 0.703 \\ 70.3 \\ 0.0502 \end{pmatrix} \quad \text{and} \quad z_{BC,0} = \begin{pmatrix} 0.0414 \\ 66.23 \\ 0.497 \end{pmatrix}$$

respectively. The computational domain is 1000ft long. We consider discretizations of 50, 100, 200, and 400 nodes respectively. In order to satisfy CFL conditions, we pick a time step of 0.05 days. Pressure, component density and saturation plots are compared with results from Transgenstein and Bell [19] as well as from Karimi et al. [8] at 150 days. Other variables are given by:

- Rock Permeability $K = 0.6328$ md.
- Porosity $\phi(p) = 0.2(1 + 10^{-5}p)$
- Relative Permeability

$$k_{r_l}(\mathbf{z}, p) = (1 - s_v(\mathbf{z}, p) - s_a(\mathbf{z}, p))(1 - s_v(\mathbf{z}, p))(1 - s_a(\mathbf{z}, p))$$

$$k_{r_v}(\mathbf{z}, p) = (s_v(\mathbf{z}, p))^2$$

$$k_{r_a}(\mathbf{z}, p) = (s_a(\mathbf{z}, p))^2$$

- Solution Ratios

$$R_l(p) = 0.05p$$

$$R_v(p) = 9 \times 10^{-5} - 6 \times 10^{-8}p + 1.6 \times 10^{-11}p^2$$

$$R_a(p) = 0.005p$$

- Viscosities

$$\mu_l(p) = 0.8 - 10^{-4}p \qquad \text{(Saturated Liquid)}$$

$$\mu_v(p) = 0.012 + 3 \times 10^{-5}p$$

$$\mu_a = 0.35 \qquad \text{(Saturated Aqua)}$$

- Volume Formation Factors

$$B_l(p) = 1.0 + 1.5 \times 10^{-4}p \qquad \text{(Saturated Liquid)}$$

$$B_v(p) = \frac{1}{6.0+0.06p} \qquad \text{(Saturated Vapor)}$$

$$B_a(p) = 1.0 - 3 \times 10^{-6}p \qquad \text{(Saturated Aqua)}$$

In order to test the robustness of our simulation, we investigate the effects of changing values of variables for which we can predict the outcome and the effects of changing initial and boundary conditions. Small modifications are made to initial

and boundary conditions so as to remain in the case of the saturated black-oil model. These changes and the associated numerical results are documented in the results section.

4.2 Results and discussion

4.2.1 Saturated black-oil model results

Figure 4.1 shows the saturation plots for the saturated black-oil case. In each subplot, the bottom curve corresponds to the vapor saturation and the top curve is the sum of vapor and liquid saturations. The distance between the top and the bottom curve is the liquid saturation, whilst the distance between one and the top curve gives the aqua saturation. These plots are the same as the ones obtained in the Tragenstein and Bell [19] and Karimi et al. [8] papers. This validates our implementation of the Kurganov Tadmor scheme and resulting simulation. In addition, we have thus confirmed that the Kurganov-Tadmor scheme results in the Karimi et al. paper are reproducible.

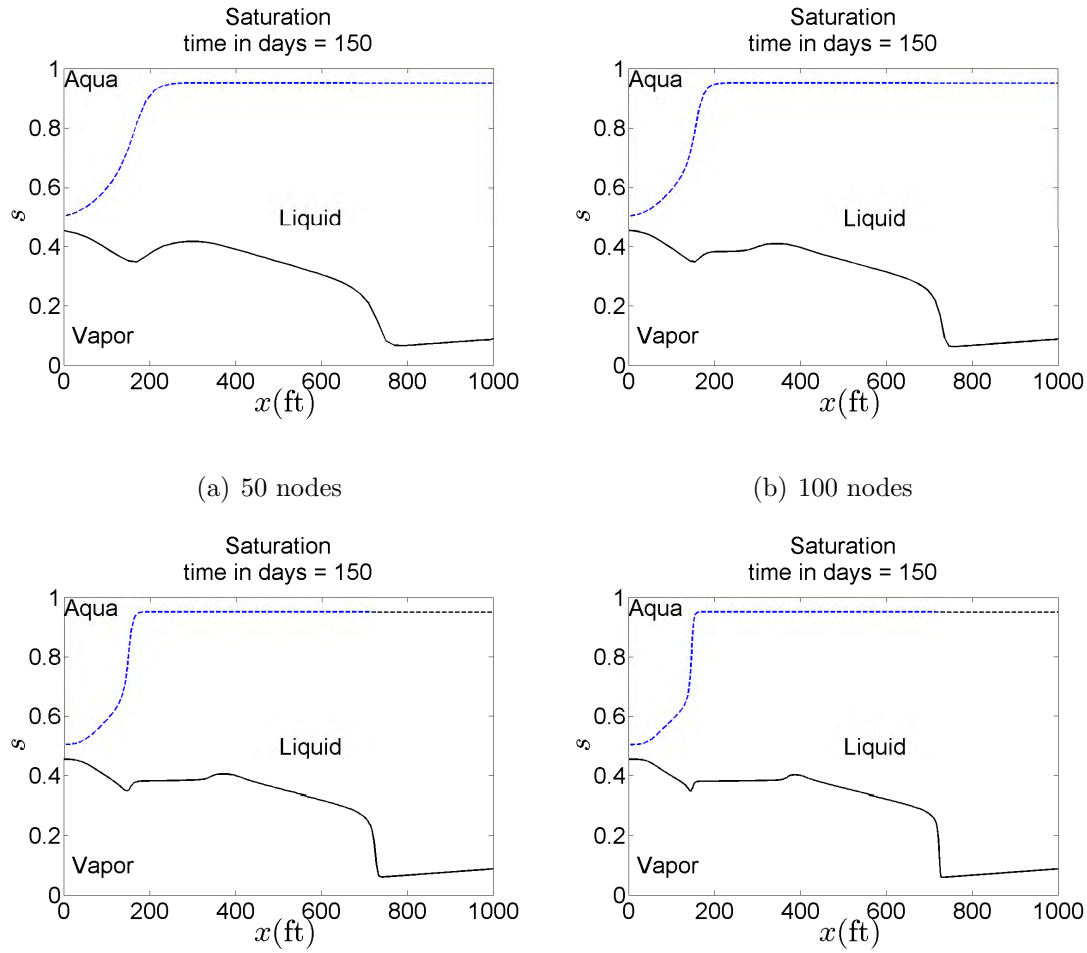

(a) 50 nodes

(b) 100 nodes

(c) 200 nodes

(d) 400 nodes

Figure 4.1 : Saturation profiles after 150 days for various number of nodal points.

Further evidence that confirms our implementation of the Kurganov Tadmor scheme includes the component density plots at 150 days using 400 nodes provided in figure (4.2). These are the same plots generated from the Transgestein and Bell paper [19].

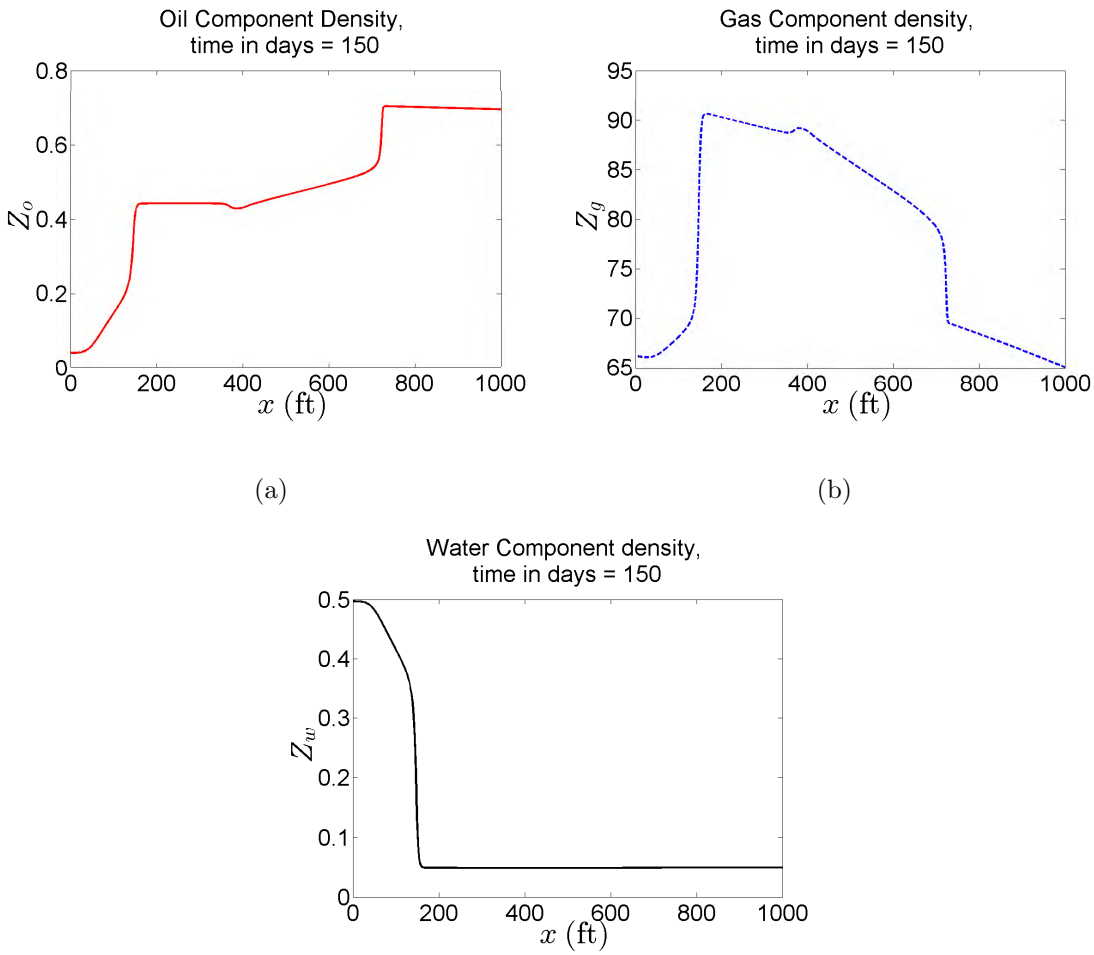

(a) (b)

(c)

Figure 4.2 : Component densities after 150 days.

4.2.2 Results for changing rock permeability

In this test case we investigate the effects of changing the rock permeability K. We test on values of $K = 0.06328$ md, and $K = 1.0$ md. Changing the value of the rock permeability affects the phase mobility and therefore the speed at which the solution propagates. Physically, decreasing the rock permeability corresponds with reducing

the pore connectivity in the reservoir. Intuitively, this will result in a slower speed of propagation. In figure (4.3) we show the slow moving saturation profile. At 150 days the saturation does not match the one in figure (4.1); however, at 1500 days we finally arrive at the matching profile.

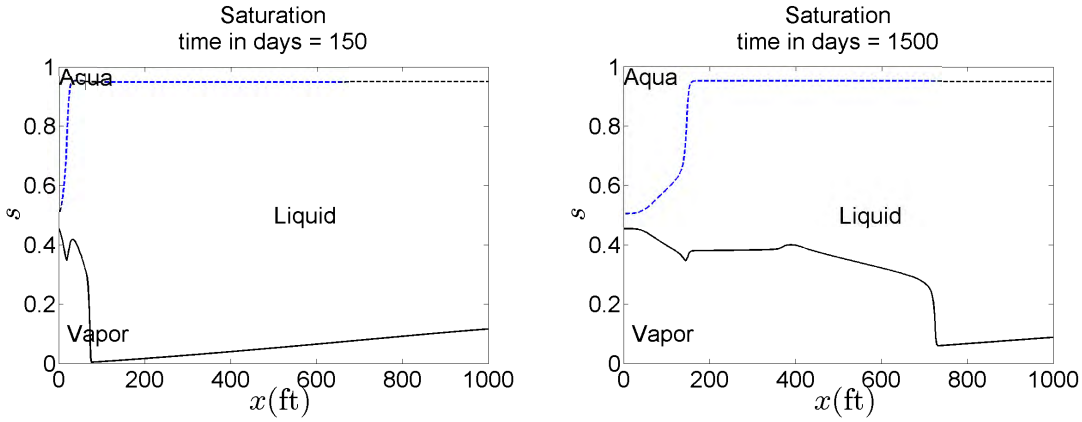

(a) 150 days

(b) 1500 days

Figure 4.3 : Saturation profiles with $K = 0.06328$md. Figures 3(a) and 3(b) illustrate the slow movement of the saturation profile at low rock permeability values K as predicted.

An increase in the rock permeability results in a faster moving profile as shown in figure (4.4).

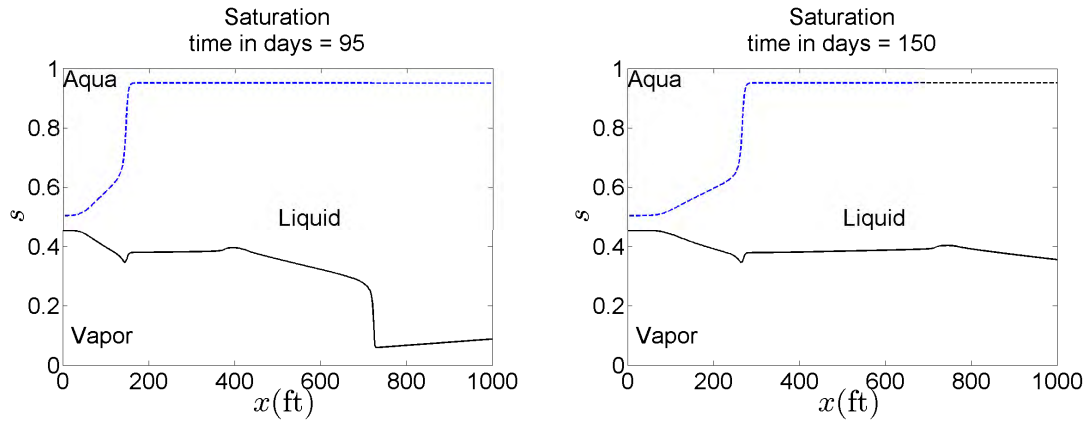

(a) 95 days

(b) 150 days

Figure 4.4 : Saturation profiles with $K = 1.0$md. Figures illustrate the fast paced saturation profile as predicted.

4.2.3 Results for changing initial conditions

We assume that at initial conditions there is no water in the reservoir. Keeping all the other variables constant in the saturated case, we consider the following initial component densities:

$$z_{IC} = \begin{pmatrix} 0.703 \\ 70.3 \\ 0.0 \end{pmatrix}.$$

The shape of the saturation profile does not change (figure 4.6), but we note that at 150 days all the water in the reservoir is concentrated between 0 ft and 190 ft (figure 4.6c). The water being injected into the reservoir has not yet propagated further into the reservoir; therefore, only oil and gas fill the reservoir from 190ft to 1000ft.

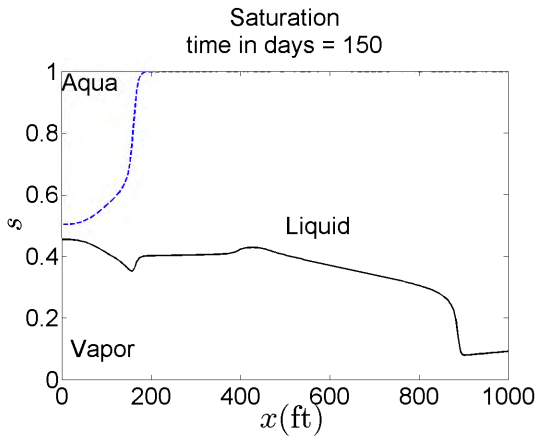

Figure 4.5 : Saturation profile after 150 days (different initial conditions).

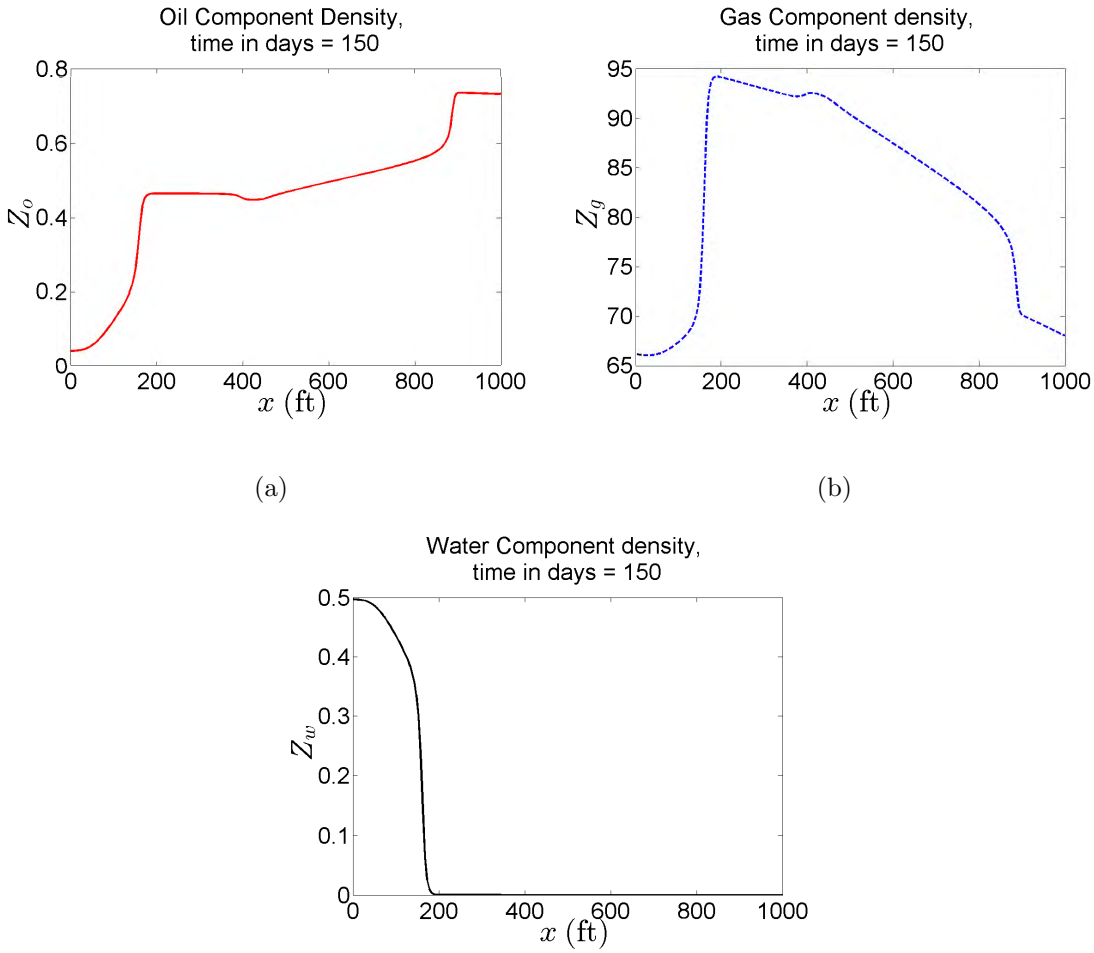

(a) (b)

(c)

Figure 4.6 : Component densities after 150 days (different initial conditions).

4.2.4 Results for changing boundary conditions

We simulate the case for which no oil is added to the reservoir in the injection process of the secondary recovery phase. Keeping all the other variables constant in the

saturated case, the injection component densities are given by:

$$z_{BC,0} = \begin{pmatrix} 0.0 \\ 66.23 \\ 0.497 \end{pmatrix}.$$

Without any oil being injected into the reservoir, the saturation and component densities retain the same plot shapes at 150 days. There are slight changes in the component densities close to the 0ft boundary, but overall having no oil injected does not affect the results of the saturated black-oil model.

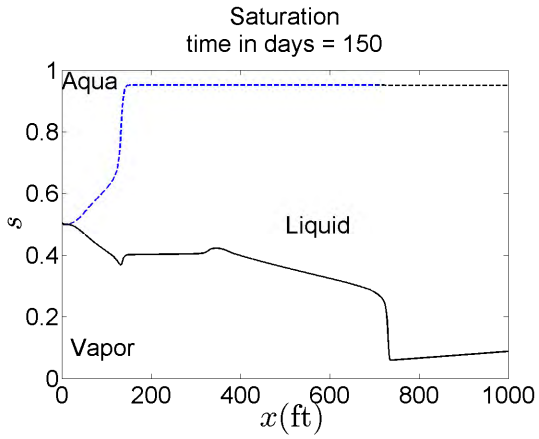

Figure 4.7 : Saturation profile after 150 days (different boundary conditions).

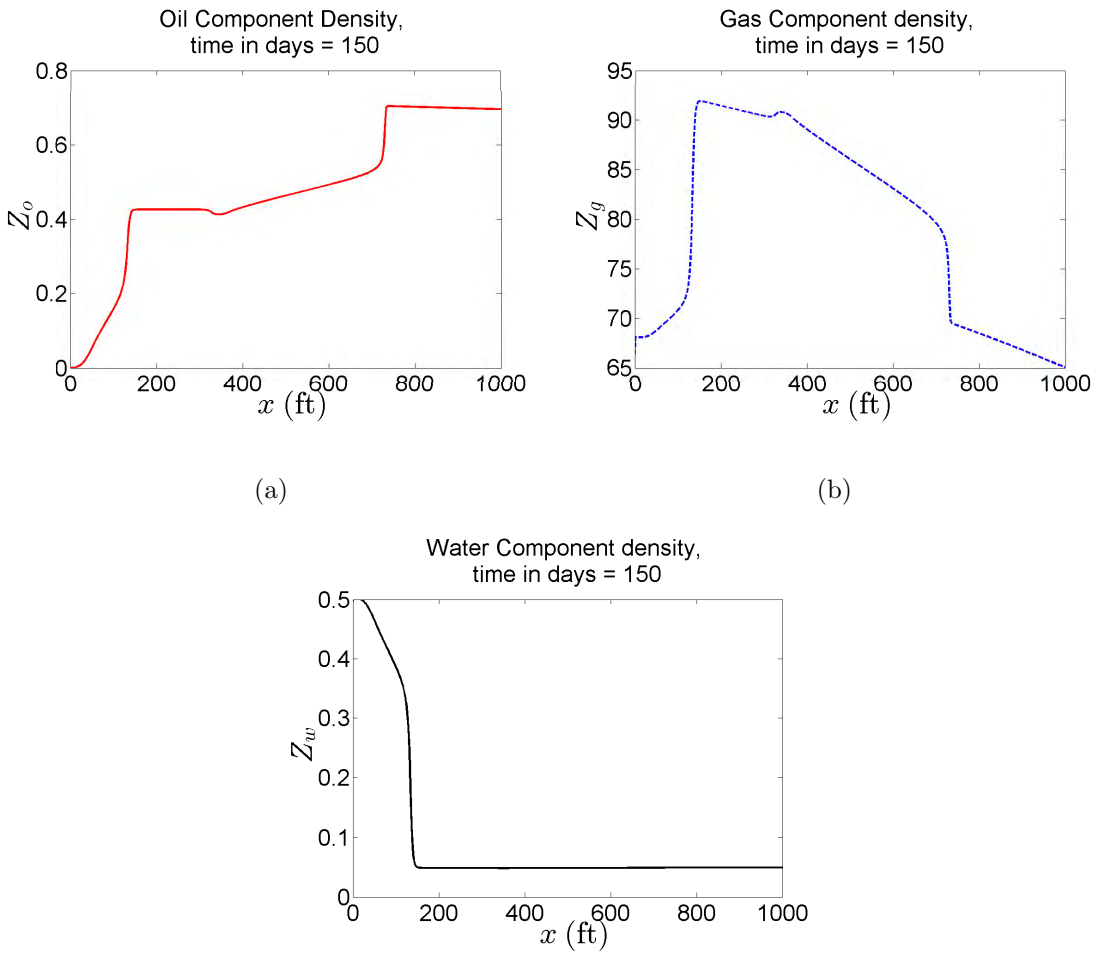

(a) (b)

(c)

Figure 4.8 : Component densities after 150 days (different boundary conditions).

Chapter 5

Conclusion

In this thesis we obtained numerical convergence rates for the Kurganov-Tadmor scheme applied to a few selected hyperbolic conservation laws. Whilst theoretical results for the convergence of the Kurganov-Tadmor scheme do not currently exist, we were able to verify second order convergence in the L^1 norm. We presented a detailed formulation for the Kurganov-Tadmor scheme applied to the saturated black-oil model given by Transgestein and Bell. This formulation allowed us to develop a simulation and compare our results with Karimi et al. The reproducibility of results from Karimi et al. strengthens the case for using the Kurganov-Tadmor scheme on the black-oil model. We were able to test the robustness of our simulation by making slight modifications to the main saturated black-oil test case.

Further areas of development include validating the implementation of the Kurganov-Tadmor scheme to the undersaturated black-oil model, applying the Kurganov-Tadmor scheme to other multi-phase multi-component fluid flow models, and extending the application of the Kurganov-Tadmor scheme to the multi-dimensional black-oil model. This work is a stepping stone to all these areas.

Bibliography

[1] K. Aziz and A. Settari. *Petroleum reservoir simulation*. Applied Science Publ. Ltd., London, UK, 1979.

[2] J. B. Bell, P. Colella, and J. A. Trangenstein. Higher order godunov methods for general systems of hyperbolic conservation laws. *Journal of Computational Physics*, 82(2):362–397, 1989.

[3] J. B. Bell, G. R. Shubin, et al. Higher-order godunov methods for reducing numerical dispersion in reservoir simulation. In *SPE Reservoir Simulation Symposium*. Society of Petroleum Engineers, 1985.

[4] G. Chavent and J. Jaffré. *Mathematical models and finite elements for reservoir simulation: single phase, multiphase and multicomponent flows through porous media*. Elsevier, 1986.

[5] R. E. Ewing. *The mathematics of reservoir simulation*. SIAM, 1983.

[6] S. K. Godunov. A difference method for numerical calculation of discontinuous solutions of the equations of hydrodynamics. *Mat. Sb. (N.S.)*, 47(89)(3):271–306, 1959.

[7] A. Harten, P. D. Lax, and B. Leer. On upstream differencing and godunov-type schemes for hyperbolic conservation laws. *SIAM review*, 25(1):35–61, 1983.

[8] A. Karimi, H. Naderan, M. T. Manzari, and S. K. Hannani. A comparison between high-resolution central and godunov-based schemes for the black-oil simulation. *International Journal of Numerical Methods for Heat & Fluid Flow*, 19(2):125–145, 2009.

[9] S. Konyagin, B. Popov, and O. Trifonov. On convergence of minmod-type schemes. *SIAM journal on numerical analysis*, 42(5):1978–1997, 2005.

[10] A. Kurganov and D. Levy. A third-order semidiscrete central scheme for conservation laws and convection-diffusion equations. *SIAM Journal on Scientific Computing*, 22(4):1461–1488, 2000.

[11] A. Kurganov and E. Tadmor. New high-resolution central schemes for nonlinear conservation laws and convection-diffusion equations. *Journal of Computational Physics*, 160:241–282, 2000.

[12] P. D. Lax. Weak solutions of nonlinear hyperbolic equations and their numerical computation. *Communications on Pure and Applied Mathematics*, 7(1):159–193, 1954.

[13] R. J. Leveque. *Finite Volume Methods for Hyperbolic Problems*. Cambridge University Press, Cambridge, 1st edition, 2002.

[14] C. Lin. New high-resolution central-upwind schemes for nonlinear hyperbolic conservation laws. In *Hyperbolic Problems: Theory, Numerics, Applications*, pages 705–715. Springer, 2003.

[15] X. Liu and E. Tadmor. Third order nonoscillatory central scheme for hyperbolic conservation laws. *Numerische mathematik*, 79(3):397–425, 1998.

[16] O. Mehmetoglu and B. Popov. Maximum principle and convergence of central schemes based on slope limiters. *Mathematics of Computation*, 81(277):219–231, 2012.

[17] H. Naderan, M. T. Manzari, and S. K. Hannani. Application and performance comparison of high resolution central schemes for black oil model. *International Journal of Numerical Methods for Heat & Fluid Flow*, 17(7):736–753, 2006.

[18] H. Nessyahu and E. Tadmor. Non-oscillatory central differencing for hyperbolic conservation laws. *Journal of Computational Physics*, 87(2):408–463, 1990.

[19] J. A. Trangenstein and J. B. Bell. Mathematical structure of the black-oil model for petroleum reservoir simulation. *SIAM Journal of Applied Mathematics*, 49(3):115–139, 1989.